Available online at www.sciencedirect.com
SCIENCE DIRECT®
Journal of Power Sources xxx (2006) xxx–xxx
JOURNAL OF POWER SOURCES
www.elsevier.com/locate/jpowsour

Synthesis and characterization of non-noble nanocatalysts for hydrogen production in microreactors

Krithi Shetty [a], Shihuai Zhao [a], Wei Cao [a], Upali Siriwardane [b], Naidu V. Seetala [c], Debasish Kuila [a,b,*]

[a] *Institute for Micromanufacturing, Louisiana Tech University, United States*
[b] *Chemistry Program, Louisiana Tech University, United States*
[c] *Department of Physics, Grambling State University, United States*

Received 18 January 2006; received in revised form 20 April 2006; accepted 21 April 2006

Abstract

Nanoscale Co and Ni catalysts in silica were synthesized using sol–gel method for hydrogen production from steam reforming of methanol (SRM) in silicon microreactors with 50 μm channels. Silica sol–gel support with porous structure gives high surface area of 452.35 $m^2 g^{-1}$ for Ni/SiO_2 and 337.72 $m^2 g^{-1}$ for Co/SiO_2. TEM images show the particles size of Ni and Co catalysts to be <10 nm. The EDX results indicate Co and Ni loadings of 5–6 wt.% in silica which is lower than the intended loading of 12 wt.%. The DTA and XRD data suggest that 450 °C is an optimum temperature for catalyst calcination when most of the metal hydroxides are converted to metal oxides without significant particle aggregation to form larger crystallites. SRM reactions show 53% methanol conversion with 74% hydrogen selectivity at 5 μL min^{-1} and 200 °C for Ni/SiO_2 catalyst, which is higher than those for Co/SiO_2. The activity of the metal catalysts decrease significantly after SRM reactions over 10 h, and it is consistent with the magnetization (VSM) results indicating that ~90% of Co and ~85% of Ni become non-ferromagnetic after 10 h.

Keywords: Microreactor; Non-noble catalysts; Silica; Methanol; Hydrogen production; Steam reforming; Magnetic properties

1. Introduction

Hydrogen production is getting a lot of attention from today's researchers due to consumption of gasoline and environmental concern. Steam reforming is an alternative process to produce hydrogen from organic sources with the aid of a catalyst [1]. Of many candidates being considered for hydrogen fuel sources, methanol, ethanol, gasoline, and diesel are four of the best candidates which are readily available, and currently being investigated [2–9]. The use of methanol for steam reforming is attractive due to its high energy density, low cost, easy transportation, and low reforming temperature. The main reactions involved in steam reforming of methanol may be presented by the following equations.

- Steam reforming of methanol:

$$CH_3OH + H_2O \rightleftarrows 3H_2 + CO_2, \quad \Delta H_r = 49.5\,kJ\,mol^{-1} \qquad (1)$$

- Methanol decomposition:

$$CH_3OH \rightleftarrows 2H_2 + CO, \qquad \Delta H_r = 90.6\,kJ\,mol^{-1} \qquad (2)$$

- Water-gas shift reaction:

$$CO + H_2O \rightleftarrows H_2 + CO_2, \qquad \Delta H_r = -41.2\,kJ\,mol^{-1} \qquad (3)$$

Considerable work already exists in literature on catalytic steam reforming of methanol for hydrogen production using conventional macroscale reactors [10–12]. However, the use of microreactors for steam reforming of methanol is relatively unexplored [8,13,14]. Recently, Kothare and his coworkers have used a microreactor with microchannels in range of 200–400 μm deep with a width of 1000 μm [8]. The advan-

* Corresponding author. Tel.: +1 318 257 5121; fax: +1 318 257 5104.
E-mail address: dkuila@latech.edu (D. Kuila).

0378-7753/$ – see front matter © 2006 Published by Elsevier B.V.
doi:10.1016/j.jpowsour.2006.04.130

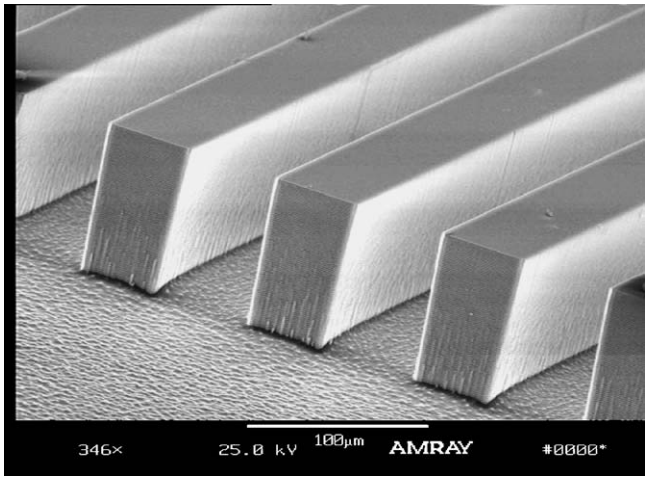

Fig. 1. SEM image of 50 μm channels in a silicon microreactor fabricated at the Institute for Micromanufacturing of Louisiana Tech.

tages of microreactor systems include lightweight, compactness, rapid heat and mass transport due to large surface to volume ratio, and precise control of process conditions with higher product yields [15]. Also, microchannel reactors working under laminar flow conditions show low-pressure drop compared to random packed bed reactors. The short radial diffusion time in microreactors leads to narrow residence time distribution of reaction gases, which allows an optimum contact time between reactants and catalysts avoiding formation of unwanted by-products.

A number of commercial and research-derived noble metals (such as Pt and Rh) loaded onto metal oxide supports (such as CeO_2, ZnO, MgO, Al_2O_3, SiO_2, ZrO_2, and TiO_2) including more than one type of catalyst-support have been tested for hydrogen production from methanol and ethanol [2–5]. The catalyst performance is greatly influenced by the type of supports. Although a number of catalysts including Cu and Pd have shown promising results, problems with deactivation of the catalysts with an ensuing decrease in hydrogen and carbon dioxide and an increase in carbon monoxide production have been reported [4]. Currently, there is little understanding of these catalysts behavior in steam reforming reactions carried out in microreactors. In addition, the noble metal catalysts are expensive. Thus, more basic research is necessary to find the optimized combination of catalyst and support for hydrogen production. This paper focuses on the development of Ni and Co non-noble nanocatalysts on silica support in microchannel reactors for SRM reactions to produce hydrogen.

2. Experimental

2.1. Microreactor fabrication and packaging

The microreactor is a silicon-based micro-device with the dimension of 1.6 cm × 3.1 cm. It consists of *via*s, feed inlet, product outlet, and reaction zone with 120 straight channels of 50 μm width and 100 μm depth (Fig. 1), and a total volume of 9.6 mm^3. The design of multi-inlets and outlets is to allow uniform distribution of reaction and product gases passing through the microchannels. The microreactor was fabricated using microelectromechanical systems (MEMS) process, photolithography and inductive coupled plasma (ICP) etching [16,17]. Anodic bonding of microreactor with Pyrex glass protects the catalysts from the environment and avoids leakage of reactants. Further details of reactor microfabrication can be found in our previous paper [18].

2.2. Catalyst preparation, coating and activation

The silica supported Co or Ni nanocatalysts were prepared by a sol–gel procedure as described below. Tetraethyl orthosilicate (TEOS), water, ethanol and nitric acid were used in preparation of silica sol–gel with the molar ratios of 1:12:45:0.26, respectively [19]. Since ethanol and water are completely miscible, a clear solution is obtained when they are mixed in appropriate quantities. TEOS was slowly added to the solution with constant stirring after the required amount of nitric acid was added. The final solution was stirred at 40–50 °C for about 30 min and allowed to age for 2 weeks. Solution of cobalt nitrate or nickel nitrate dissolved in water was added with intended loadings (12% for either Co or Ni) to the silica sol. After the catalyst solution was completely dissolved in the sol, it was coated into reactor microchannels using drop-coating method. The sol–gel coated microreactor was dried by gentle heating, where polycondensation leads to cross-linking and polymerization of silica, and treated with 10% NH_4OH solution for 30 min to form hydroxides of metal catalysts, followed by washing with DI-water to remove residuals from ammonia treatment, and drying in a vacuum oven for 30 min at 60 °C. Calcination at 450 °C for 4 h completed formation of oxides from hydroxides. The oxides of cobalt and nickel were finally reduced to active metals in a continuous flow of 40% hydrogen (nitrogen as balance for safety consideration) at 450 °C for 4–6 h before packaging of the microreactor. Any oxidation of catalysts that might have occurred during packaging and mounting of the microreactor was eliminated by further *in situ* hydrogenation for additional 2 h prior to SRM reactions.

2.3. Characterization of nanocatalysts with supports

Amray 1830 Scanning Electron Microscope (SEM) along with Energy Dispersive X-ray (EDX) was used to study uniformity and elemental composition of silica supported catalysts deposited in microchannel reactors. LIBRA 120 Carl Zeiss Transmission Electron Microscope (TEM) was used to estimate the particles size of the nanocatalysts in silica. Specific surface area (SSA) and pore size analysis of the silica supported catalysts were done using Brunaur-Emmett-Teller (BET) method with Quantachrome NOVA 2000 analyzer. Shimadzu DTA-50 differential thermal analyzer (DTA) was used to optimize the catalyst calcination temperature. Phase identification was carried out using Scintag Inc. powder X-ray diffractometer (XRD). The magnetization studies of the silica supported Co and Ni catalysts in microreactors were performed before and after SRM reactions using 880A Digital Measurement Sys-

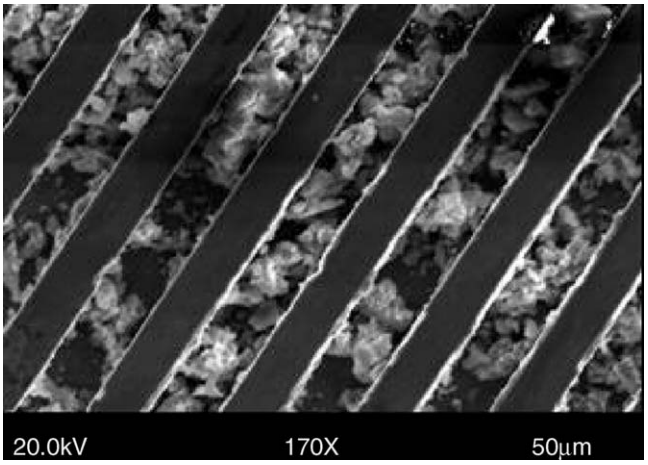

Fig. 2. SEM image of Co/SiO_2 nanocatalyst coated in 50 μm channels.

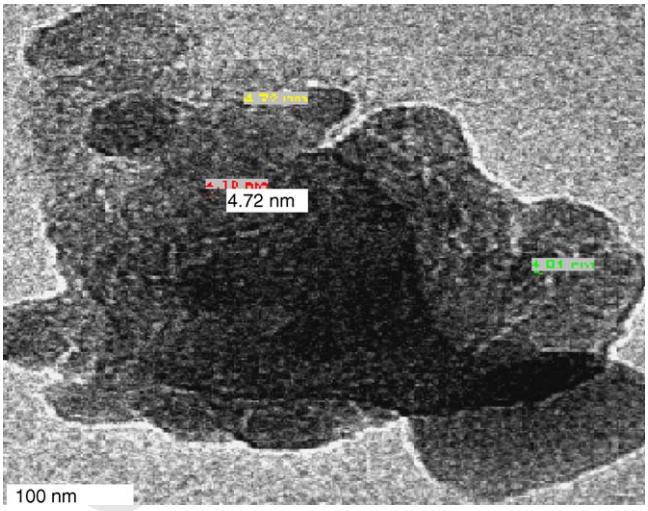

Fig. 3. TEM image of Co nanoparticles in silica synthesized by sol–gel method.

tems Vibrating Sample Magnetometer (VSM) to determine the reduction efficiency and chemical changes of Co and Ni catalysts.

2.4. Experimental setup for catalytic SRM reaction

SRM reactions were conducted using silicon-based microreactors at 180–240 °C under atmospheric pressure. Flow rates of 1:1 methanol/water between 5 and 20 $\mu L\,min^{-1}$ were controlled in the microreactors using a syringe pump. The reaction temperature was controlled using a hot plate. A cold trap was used to separate gaseous products from aqueous methanol and water. Methanol conversion was calculated from volume difference between the fed methanol–water mixture and the unreacted methanol–water mixture cooled with liquid N_2 in the trap. The gaseous products containing H_2, CO_2 and CO were diluted with helium and analyzed using a Mass Spectrometer (MS) coupled with a residual gas analyzer (RGA) (QMS 200 Gas Analyzer from Stanford Research Systems). Hydrogen selectivity was calculated on the basis of partial pressures (proportional to moles) of different products:

$$H_2 \quad \text{selectivity} = \frac{\text{partial pressure of } H_2/\text{sum of partial pressures } (H_2 + CO + CO_2)}{} \quad (4)$$

3. Results and discussion

3.1. Structure and composition of sol–gel supported nanocatalysts in microreactors

SEM imaging of the microchannels with the silica encapsulated catalysts was performed to monitor the deposition of sol–gel in the microchannels. Fig. 2 shows that silica sol–gel supported Co catalyst does not form an uniform film on the walls of microchannels. However, the microchannels are not clogged as free gas flow was observed during SRM reactions. Current work is in progress to determine the optimum coating method to make better film of supported catalysts in the microchannels. The elemental analysis done on the nano metal catalysts indicate all chemical forms of the catalysts: pure metallic, oxides and any nitrate salt that is left without reduction. It is concluded that both Ni and Co catalysts in the microchannels show loadings of 5–6%, which are much lower than intended loadings of 12%. This may be due to loss of nickel and cobalt salts during ammonia wash. The EDX analysis at different locations of the sample shows uniform distribution of the catalyst in sol–gel matrix. From TEM image (Fig. 3), we can estimate the size of the Co-particles in silica sol–gel to be <10 nm.

3.2. Surface area and pore size of silica supported nanocatalysts

The pore size and surface area properties of Ni and Co nanocatalysts incorporated with silica sol–gel matrix are shown in Table 1. As surface area of a catalyst significantly affects chemical reaction rate, surface area measurement is critical. Since the amount of sol–gel maintained in a microreactor is too small to perform BET surface area analysis, specific surface area (SSA) was analyzed with a certain amount of silica sol–gel supported nickel or cobalt catalyst prepared under similar conditions. As seen from Table 1, Ni catalyst has much higher SSA than Co catalyst. With SiO_2 porous structure, Ni and Co can be effectively distributed to obtain larger surface area available for catalytic SRM reactions.

Table 1
Surface area and pore size analyses of Co/SiO_2 and Ni/SiO_2 nanocatalysts

	Specific surface area ($m^2\,g^{-1}$)	Pore volume ($cc\,g^{-1}$)	Pore diameter (Å)
Co/SiO_2	337.72	0.1192	31.790
Ni/SiO_2	452.35	0.2392	31.790

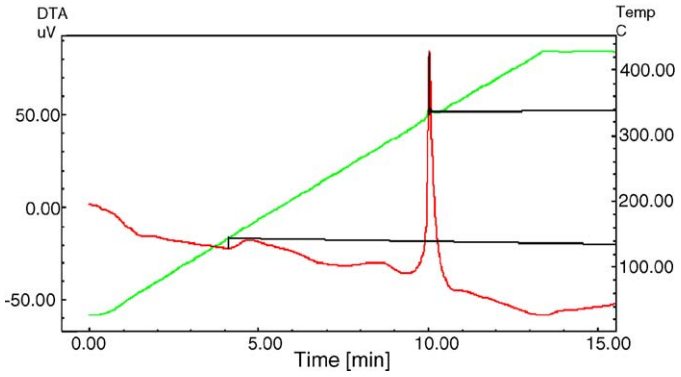

Fig. 4. Differential thermal analysis of nickel–silica catalyst.

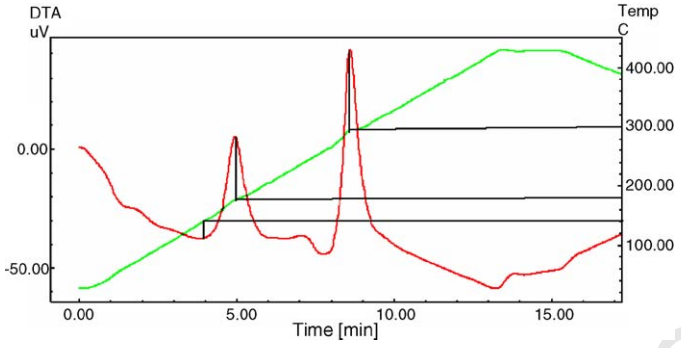

Fig. 5. Differential thermal analysis of cobalt–silica catalyst.

3.3. Optimization of catalyst calcination temperature

The optimization of calcination temperature was obtained by DTA. For both Ni/SiO_2 (Fig. 4) and Co/SiO_2 (Fig. 5), endothermic peaks were observed at ~100 °C which can be attributed to evaporation of water [20,21]. Due to ammonia treatment during synthesis of the sol–gel encapsulated catalysts, most of metal nitrate salts are converted to metal hydroxides which are further converted to metal oxides from heating in air. The broad endothermic peaks observed at 100–150 °C can be considered as water loss and some of the metal nitrate salts getting decomposed for both Ni and Co catalysts [20]. Two exothermic peaks observed for Co and one for Ni may be either due to the metal hydroxides getting converted to the oxides or due to structural changes of the surface species [22]. Thus, it may be concluded from Figs. 4 and 5 that all of the metal hydroxides are converted to the metal oxides in temperature range of 350–400 °C, which can be considered the minimum temperature for calcination before hydrogenation of the metal oxides. There were no significant thermal changes between 400 and 1000 °C indicating complete calcination of the catalysts.

Figs. 6 and 7 show the XRD patterns at room temperature for Ni/SiO_2 and Co/SiO_2 annealed at 450 and 1000 °C. Pure silica sol–gel heated to 1000 °C shows sharp peak at $2\theta = 22°$ that matches with that of pure crystalline silicon oxide (ICDD# 10-1170 tridymite) [23]. However, when a metal oxide is incorporated in it, the 22° sharp peak broadens corresponding to amorphous silica matrix [23]. This peak also suggests densification of the glass matrix. As the sample temperature is increased from 450 to 1000 °C, sharpness and intensity of the peaks also increase due to formation of larger crystallites. This represents evolution of the particle size and corresponds well to crystal growth.

The diffraction peaks of NiO observed in Fig. 6 show higher crystalline characteristics for samples calcined at 1000 °C than that at 450 °C. This indicates that heating the catalysts at very high temperatures may result in large crystallite sizes due to aggregation. It has been reported that NiO crystallite in small size favors large Ni surface area after reduction [24]. This implies that higher calcination temperature is not preferred for nanocatalysts. The XRD pattern of Co/SiO_2 heated at 450 °C in Fig. 7 shows low signal to noise ratio due to low crystallinity of the sample at low temperature. The XRD pattern at 1000 °C shows the presence of sharp peaks indicating formation and coexistence of larger crystalline particles of two chemical forms of cobalt oxides, Co_3O_4 (ICDD# 42-1467) and Co_2O_3 (ICDD# 02-0770). These two species correspond to two peaks of DTA in Fig. 5 and are consistent with the findings reported elsewhere [25,26]. From DTA and XRD studies, we selected 450 °C as the optimized calcination temperature for both Ni and Co catalysts.

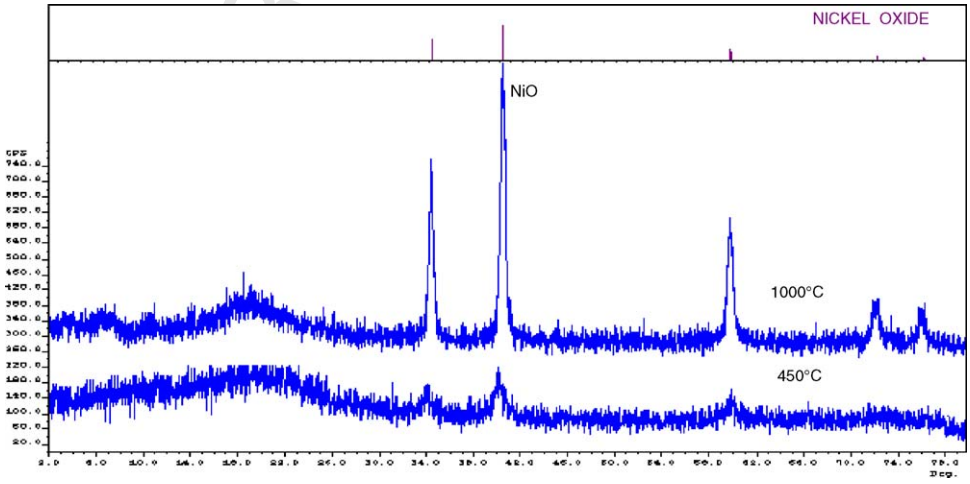

Fig. 6. X-ray diffraction patterns of Ni/SiO_2 catalyst heated at 450 and 1000 °C.

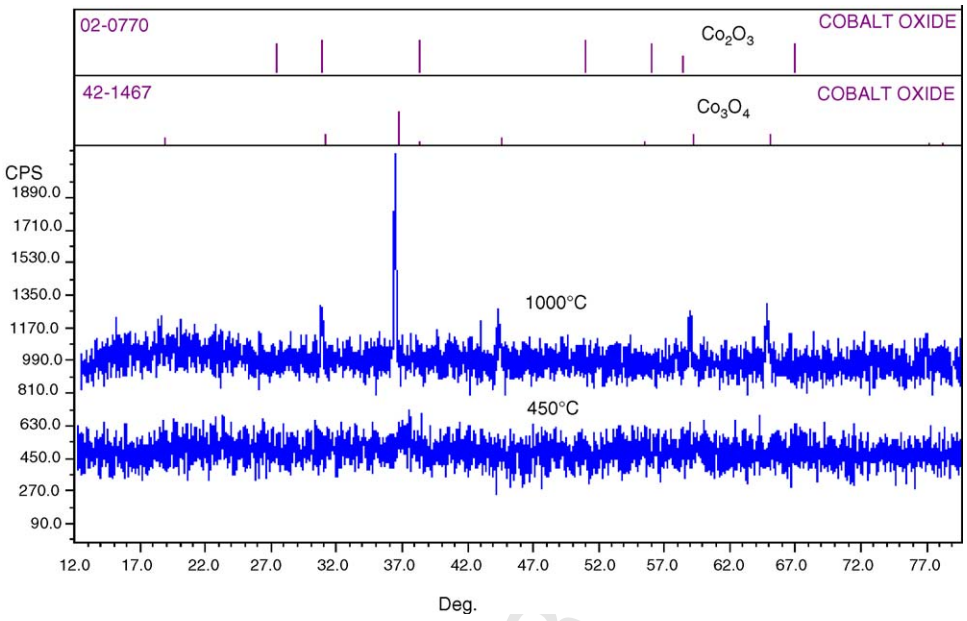

Fig. 7. X-ray diffraction patterns of Co/SiO_2 catalyst heated at 450 and 1000 °C.

3.4. Magnetization results of nanocatalysts

Since pure metallic Co and Ni are ferromagnetic, it is useful to study magnetic behavior of Co and Ni catalysts to understand the reduction efficiency during hydrogenation and chemical compound formation of metal catalysts during catalytic reactions. The saturation magnetization of the ferromagnetic component in magnetic curves obtained from VSM was used along with the EDX results to estimate the pure metallic Co and Ni in the catalysts.

Magnetization studies of the silica supported Co catalyst in microreactors were performed before and after SRM reaction. The magnetization studies for Ni catalyst are presented elsewhere [27]. The magnetization curve (Fig. 8) of calcined Co catalyst just before reduction with hydrogen shows paramagnetic behavior as cobalt is in its oxide forms, which is also confirmed from the XRD and DTA results. Hydrogenation of the catalyst reduces most, if not all, of the Co oxide to pure metal (the active phase for SRM reaction), thus giving the catalyst the ferromagnetic behavior. The ferromagnetic nature almost disappears in the post-reaction catalyst sample as most of the metallic Co yields non-ferromagnetic species. Hence, the magnetization results were used for ferromagnetic catalysts to estimate the pure metal content from the saturation magnetization value of the ferromagnetic component obtained at different stages [18]. The magnetization results indicate that ~33% cobalt oxide is reduced to pure Co and ~45% nickel oxide is reduced to pure Ni during hydrogenation at 450 °C for 5 h.

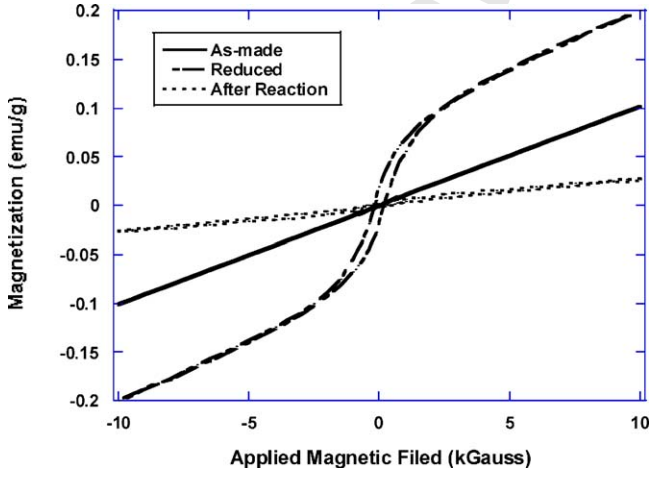

Fig. 8. Room temperature magnetization curves of Co/SiO_2 before reduction, after reduction and after SRM reaction using a vibrating sample magnetometer.

3.5. Catalytic activity for steam reforming of methanol

Methanol conversion and hydrogen production at different temperatures and flow rates of the reactants were measured over Co or Ni nanocatalyst supported by silica sol–gel in a microreactor containing 50 μm channels. A $CH_3OH:H_2O$ ratio of 1:1 was chosen for all the SRM reaction experiments. The catalytic activities for Ni and Co nanocatalysts are shown as a function of flow rate in Figs. 9 and 10, and as a function of temperature in Figs. 11 and 12. The main products of SRM reaction are hydrogen and carbon dioxide with small amount of carbon monoxide. The methanol conversion decreases as the flow rate is increased (Fig. 9) for both Co/SiO_2 and Ni/SiO_2 nanocatalysts with slightly higher conversion for Ni/SiO_2. While our ongoing studies with Ni/SiO_2 show 53% methanol conversion, Co/SiO_2 shows only 37% conversion at 5 μL min^{-1} flow rate and 200 °C. This may be attributed to larger specific surface area (Table 1) of Ni/SiO_2 catalyst [27]. However, to date, the catalysts' behavior in microreactors for SRM has been not fully discovered and understood. The decrease of methanol conversion with increasing flow rate may be explained by lower residence time of the reactants in the microreactor at higher flower

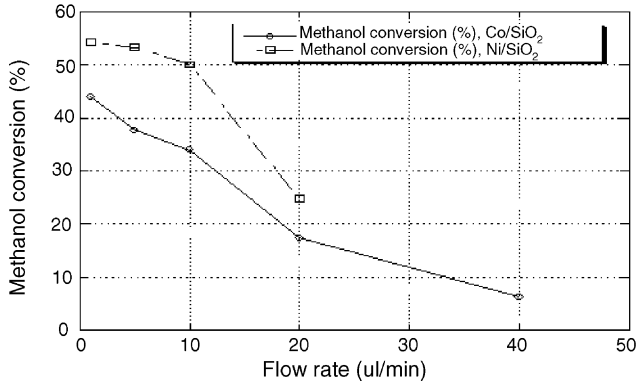

Fig. 9. Methanol conversion (CH_3OH:H_2O ratio of 1:1) as a function of flow rate at 200 °C using silica sol–gel supported Ni/SiO_2 and Co/SiO_2 nanocatalysts in 50 μm channel microreactor.

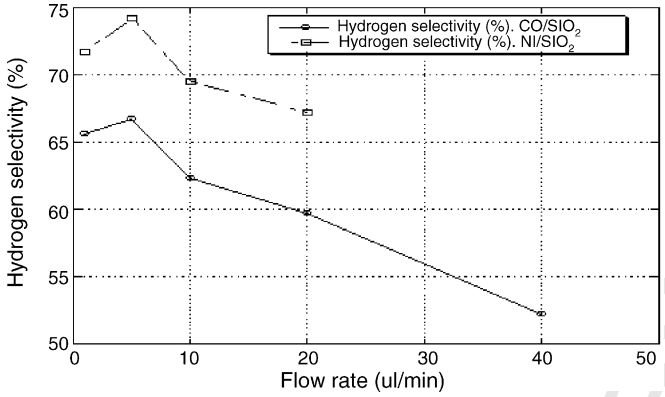

Fig. 10. Hydrogen selectivity (CH_3OH:H_2O ratio of 1:1) as a function of flow rate at 200 °C using silica sol–gel supported Ni/SiO_2 and Co/SiO_2 nanocatalysts in 50 μm channel microreactor.

rates. The hydrogen selectivity (Fig. 10) also showed similar variations (decreasing) with increasing flow rate. The maximum hydrogen selectivity is ~74% for Ni/SiO_2 catalyst and ~67% for Co/SiO_2 at 5 μL min^{-1} flow rate and 200 °C. Further, the temperature in range of 180–240 °C does not have a significant effect on methanol conversion for both catalysts (Fig. 11). However, hydrogen selectivity (Fig. 12) in both Ni/SiO_2 and Co/SiO_2 cases is affected by the variation of temperatures. The hydrogen selectivity is the maximum at 200 °C for Ni/SiO_2 catalyst and at 220 °C for Co/SiO_2 catalyst.

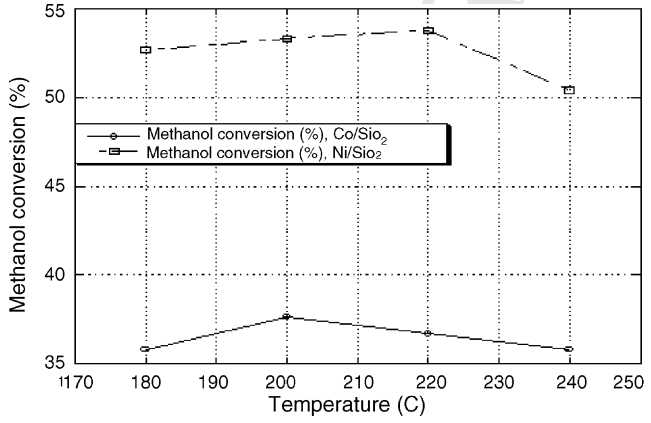

Fig. 11. Methanol conversion (CH_3OH:H_2O ratio of 1:1) as a function of temperature at a flow rate of 5 μL min^{-1} using silica sol–gel supported Ni/SiO_2 and Co/SiO_2 nanocatalysts in 50 μm channel microreactor.

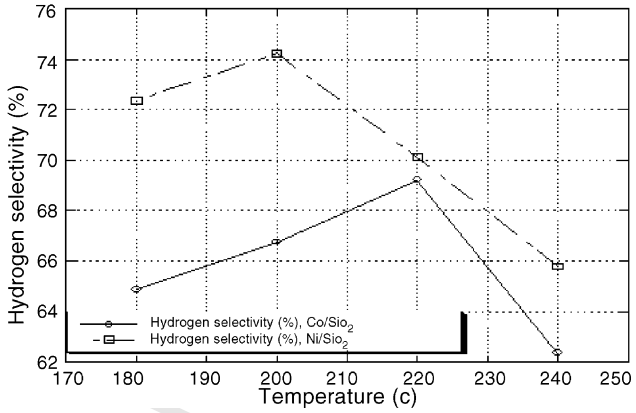

Fig. 12. Hydrogen selectivity (CH_3OH:H_2O ratio of 1:1) as a function of temperature at a flow rate of 5 μL min^{-1} using silica sol–gel supported Ni/SiO_2 and Co/SiO_2 nanocatalysts in 50 μm channel microreactor.

All the reactions described above were carried out within 8 h and no significant deactivation of the catalysts was observed during this period. However, when these reactions were carried out over 10 h, deactivation of the catalysts was noticed which is consistent with the VSM analysis. The VSM results from the post-reaction catalyst sample (see Fig. 8) provide an estimate of ~90% Co and ~85% Ni being converted to non-ferromagnetic species after SRM reactions over 10 h. These species may be Ni- or Co-compounds such as their oxides, carbonyls and carbides [28,29].

4. Conclusion

Silica supported Ni and Co nanocatalysts were synthesized by sol–gel method and coated in 50 μm channel silicon microreactors. The catalyst activity and its effect on methanol conversion and hydrogen selectivity in SRM reaction were investigated. EDX results show uniform distribution of nanocatalysts in silica matrix with actual loadings of 5–6%, which is lower than the intended loadings of 12%. The specific surface area (SSA) and pore size of Ni/SiO_2 catalyst are much higher than that of Co/SiO_2. Both Ni and Co catalysts have a particle size of <10 nm observed by TEM images. DTA and XRD studies show that 450 °C is the optimum calcination temperature for conversion of metal hydroxides to metal oxides which are subsequently reduced to metal prior to SRM reactions for both Ni and Co catalysts. Higher conversion and hydrogen selectivity were observed for Ni/SiO_2 catalyst compared to Co/SiO_2. Magnetization studies indicate that most of the nanocatalysts becomes non-ferromagnetic and shows lower activity after 10 h of SRM reactions.

Acknowledgements

The authors would like to thank Dr. J. Spaulding for the TEM image, Mr. J. Fang for the microreactor design and set-up, Mr. S.

Vudarapu for acquiring the XRD data, and Dr. K. Varahramyan for support of this work. This research was supported by NSF-EPSCoR and Louisiana BoR-RCS (Board of Regents Research Competitive Subprogram) to D. Kuila under contract No. 32-0967-40789.

References

[1] H. Kim, Int. J. Hydrogen Energy 28 (2003) 1179.
[2] A. Goula, K. Kontou, E. Tsiakaras, Appl. Catal. B 49 (2004) 135.
[3] H. Purnama, T. Ressler, E. Jentoft, H. Soerijanto, R. Schlogl, R. Schomacker, Appl. Catal. A 259 (2004) 83.
[4] V. Twigg, S. Spencer, Top. Catal. 22 (2003) 191.
[5] T. Mizuno, Y. Matsumura, T. Nakajima, S. Mishima, Int. J. Hydrogen Energy 28 (2003) 1393.
[6] X. Zhang, J. Mol. Catal. A: Chem. 194 (2003) 99.
[7] F. Frusteri, S. Freni, L. Spadaro, V. Chiodo, G. Bonura, Catal. Commun. 5 (2004) 611.
[8] V. Pattekar, V. Kothare, J. MEMS 13 (2004) 7.
[9] D. Srinivas, V. Satyanarayana, S. Potdar, P. Ratnasamy, Appl. Catal. A 246 (2003) 323.
[10] J. Amphlett, M. Evans, R. Jones, R. Mann, R. Weir, Can. J. Chem. Eng. 59 (1981) 720.
[11] P. Wild, M. Verhaak, Catal. Today 60 (2000) 3.
[12] R. Idem, N. Bakhshi, Ind. Eng. Chem. Res. 33 (1994) 2047.
[13] S. Fitzgerald, R. Wegeng, A. Tonkovich, Y. Wang, H. Freeman, J. Marco, G. Roberts, D. VanderWeil, Proceedings of Fourth International Conference Microreaction Technology, Atlanta, GA, March 5–9, 2000, p. 358.
[14] L. Makarshin, D. Andreev, V. Parmon, Proceedings of the 0International Hydrogen Energy Congress and Exhibition IHEC, Istanbul, Turkey, July 13–15, 2005, 2005.
[15] W. Ehrfeld, V. Hessel, H. Löwe, Microreactors—New Technology for Modern Chemistry, Willey–VCH, Weinheim, 2000.
[16] M. Madou, Fundamentals of Microfabrication, CRC Press, 1997, ISBN 0-8493-9451-1.
[17] R. Hill, J. Vac. Sci. Technol. B 14 (1996) 547.
[18] S. Nagineni, S. Zhao, A. Potluri, Y. Liang, U. Siriwardane, S. Naidu, J. Fang, J. Palmer, D. Kuila, Ind. Eng. Chem. Res. 44 (2005) 5602.
[19] S. Okuzaki, K. Okude, T. Ohishi, J. Non-Cryst. Solids 265 (2000) 61.
[20] H. Ming, B. Baker, Appl. Catal. A 123 (1995) 23.
[21] W. Fua, H. Yan, L. Changa, M. Li, H. Bala, Q. Yu, G. Zoua, Colloids Surf. A 262 (2005) 71.
[22] T. Daniels, Differential Thermal Analysis, Kogan Page, London, 1973.
[23] Z. Zhou, J. Xue, J. Wang, J. Appl. Phys. 91 (2002) 6015.
[24] L. Narvaez, O. Dominguez, J. Martınez, F. Ruiz, J. Non-Cryst. Solids 318 (2003) 37.
[25] O. Lima, A. Papacídero, Mater. Charact. 50 (2003) 101.
[26] N. Elbashir, P. Dutta, A. Manivannan, M. Seehra, C. Roberts, Appl. Catal. A 285 (2005) 169.
[27] K. Shetty, S. Zhao, W. Cao, N. Seetala, D. Kuila, Proceedings of Materials Research Society Conference, Boston, MA, fall, in press.
[28] M. Akundi, J. Zhang, M. Gibbs, M. Watson, A. Murty, S. Naidu, E. Bruster, L. Turner, F. Waller, IEEE Trans. Magn. 37 (2001) 2929.
[29] A. Belhekar, S. Ayyappan, A. Ramaswamy, J. Chem. Technol. Biotechnol. 59 (1994) 395.